

Received May 11, 2019, accepted June 3, 2019, date of publication June 10, 2019, date of current version June 26, 2019.

Digital Object Identifier 10.1109/ACCESS.2019.2921794

A New Adaptive Robust Unscented Kalman Filter for Improving the Accuracy of Target Tracking

WEIDONG ZHOU AND JIAJIN HOU^{ID}, (Student Member, IEEE)

Department of Automation, Harbin Engineering University, Harbin 150001, China

Corresponding author: Jiaxin Hou (houjiaxin@hrbeu.edu.cn)

This work was supported by the National Natural Science Foundation of China under Grant 61573113 and Grant 61371173.

ABSTRACT In target tracking, the tracking process needs to constantly update the data information. However, during data acquisition and transmission of sensors, outliers may occur frequently, and the model is disturbed by non-Gaussian noise, that affects the performance of system state estimation. In this paper, a new filtering algorithm is proposed based on *QR* decomposition and singular value decomposition (SVD) method, namely adaptive robust unscented Kalman filter (QS-ARUKF) to suppress the interference of outliers, non-Gaussian noise as well as a model error to achieve high accuracy state estimation. An adaptive filtering algorithm based on strong tracking idea is used in modifying the state equation of unscented Kalman filter (UKF), so that the algorithm can effectively improve the tracking ability of the state model. By using the robust filtering method to construct a new cost function used to modify the measurement covariance formula of the Kalman filter, the error of measurement model can be effectively suppressed. The *QR* decomposition is introduced to the time update and measurement update to avoid the covariance non-positive definite. We propose the SVD method to address the problem of numerical sensitivity in the filtering process. The purpose of this method is to replace the calculation of the inverse of the filter gain matrix and further improve the robustness of the algorithm. The simulation results showed that the proposed algorithm has higher accuracy and better robustness than the traditional filtering method.

INDEX TERMS Nonlinear system, unscented Kalman filter (UKF), nonlinear filtering, adaptive robust Kalman filter.

I. INTRODUCTION

State estimation for nonlinear dynamic systems has attracted great attention in control and signal processing. Filtering algorithms play an important role in dealing with nonlinear systems, including some classical algorithms: such as extended Kalman filter (EKF), central difference Kalman filter (CDKF), subsequent Gaussian-Hermite filter (GHF), cubature Kalman filter (CKF), unscented Kalman filter (UKF) and particle filter (PF). These algorithms have been widely used in navigation and control [1]–[7], missile target tracking [8]–[10], video tracking [11]–[13] and lithium battery performance evaluation [14], [15]. Kalman filter (KF) is a filtering method based on linear least squares [16], [17], however, the core idea of nonlinear filtering is an approximate estimation, which is a suboptimal mean estimation and its performance that depends on the predefined model. Model

The associate editor coordinating the review of this manuscript and approving it for publication was Qinghua Guo.

mismatch, initial error, random noise [18], and non-Gaussian heavy-tailed noise [19]–[22] lead to the reduction or even divergence of filtering accuracy.

The essence of target tracking is nonlinear, and each system contains multiple nonlinear factors. At present, the most widely used nonlinear filter is EKF, and by approximating the first order linearization of nonlinear functions, the nonlinear filtering problem is transformed into linearization. However, under strong nonlinearity, the first-order linearization truncation and neglecting the higher-order term, bring the large error and lead to the filter divergence [23], [24]. EKF is not a good choice for dealing with strong nonlinear systems to replace traditional nonlinear estimation from the perspective of identification [25]. Recently, a very effective alternative to EKF is UKF, which has received wide attention [26]. The core idea of UKF is unscented transformation (UT), which uses the same sampling points as the system state distribution to propagate mean and (cross) covariance through non-linear mapping. UT is a kind of statistical linear regression (SLR),

regression coefficient matrix which can be regarded as the intentional approximation of Jacobian matrix and avoids the tedious calculation of the Jacobian matrix. Regardless of the degree of nonlinearity, UT theoretically approximates the posteriori mean and covariance of any nonlinear system state with second-order Taylor accuracy [27], [28]. Such as unscented information filter [29], [30], the unscented H_{oo} filter [31]–[33], and the robust UKF [34], [35]. This series shows that UT plays a vital role in the filtering algorithm. Therefore, UKF is chosen as a typical nonlinear filter owing to precision requirement and computational cost.

However, the nonlinear filters are easily affected by model mismatch, random error, and other non-ideal environments [18], [36]–[38], so they fall short in terms of adaptability and robustness. In some engineering applications, such as unreliable sensors tracking agile targets with measured outliers, heavy-tailed non-Gaussian process and measurement noises takes place [22], [39], [40]. In [41], the rolling time domain Kalman finite pulse response was used in reducing the effect of model uncertainty on the system and the transient unknown sensor bias. However, the filter is based on finite impulse response, so it is difficult to converge quickly and achieve the best filtering effect for the algorithm. In [42], although the suboptimal fading factor was introduced into the time update stage and applied to visual tracking to improve the robustness and accuracy of the algorithm, the numerical sensitivity problem has not been investigated. Zhang et al. proposed Robust-CKF based on SVD for Inertial Navigation System/Global Positioning System. The SVD method was used to replace the Cholesky decomposition of CKF, but the numerical sensitivity of the inversion of the covariance in the gain matrix has not been solved [43]. In [44], square root UKF (SRUKF) is proposed for time update and measurement update. Although the covariance was decomposed, the problem of numerical sensitivity has remained unsolved. In [45], the hypothesis test was used in identifying the system model, and the idea of strong tracking was implemented. The unknown variables are introduced into the system model. So, the prediction covariance non-positive definite, and the UKF fails. Hu and Liu proposed that the multiple fading factors were introduced to Inertial Navigation System/Global Positioning System (INS/GPS), and the abnormal state was detected [46]. The result was improved compared to the standard UKF, however, the convergence speed and computational complexity of high-dimensional state vectors have yet to be addressed. Wang et al. studied the adaptive robust UKF and applied it to satellite-integrated navigation to attenuate the interference caused by the system model uncertainty. However, the adaptive factor and equivalent weight factor in adaptive robust filtering are selected according to expert experience. Therefore, the limitation of filtering has not been solved [47]. In [48], the methods of windowing and random weighting, combined with UKF filter were used to address solve the uncertainty problem in noise statistics, but the convergence rate was slow when the state is abrupt or strongly nonlinear. To further improve the

accuracy of Kalman filtering, many scholars have focused on the problem of outliers. In [13], no derivative filter was proposed to control the outliers, and suppressing the state mutation was inadequate. In the case of disturbance uncertainties, the performance of the M-estimation method that deals with measurement outliers decreases when both the state model and measurement model are contaminated by outliers [49], [50]. In [51], the novel robust UKF was proposed based on the Huber, which was only used to modify the standard UKF measurement equation, so the influence of the state equation on the whole system is not considered. Chen et al. dealt with non-Gaussian noise in the nonlinear system but did not elaborate on the model mismatch or measurement anomalies [52]. Maximum correntropy Kalman filter (MCKF) was proposed to deal with large process uncertainty based on maximum correlation entropy, which was calculated by the correlation entropy of the maximum estimation error and residual [53]–[56]. However, the establishment of the estimation error covariance matrix lacked the theoretical basis, resulting in limited estimation accuracy.

The standard UKF needs Cholesky decomposition of the state covariance matrix at each filtering; however, the distribution of UKF weights and sampling points causes the covariance to lose positive definiteness after several updates, leading to the invalidation of the filtering results. When the filtering effect is optimal, the gain matrix remains stable. As the system model mutates, it is difficult for the gain matrix to keep up with the needed by the steady state system quickly, and this prevents the system to converge quickly. The solution of gain matrix implies the operation of inverse covariance that is the numerical sensitivity problem and also causes the filter failure. In addition, UKF is severely degraded when the kinetic model is contaminated by outliers [21], [57].

To improve the robustness of the filter, we propose a new adaptive robust unscented Kalman filter (QS-ARUKF) based on *QR* method decomposition and SVD method. The state estimation problem under state mutation and measurement anomaly and non-Gaussian noise has been studied. The *QR* method is introduced to replace Cholesky decomposition in UKF to ensure the positive covariance of the filter updating process. To reduce the weight of filter covariance in the stationary state, adjust the gain matrix of the nonlinear system, and suppress the influence of state mutation, we introduced the suboptimal fading factor based on the orthogonal principle of the residual vector into the prediction covariance matrix. The SVD method is introduced to avoid the influence of ill-conditioned covariance and numerical sensitivity on the gain matrix in the measurement update. The modified covariance matrix is used in constructing the Huber cost function to further improve the robustness of the algorithm and to ensure that the algorithm reaches the global optimum for the whole system.

This article is organized as follows: The system model and the standard UKF are introduced In Section II. In Section III, two propositions and analytical expressions of adaptive attenuation factor are given, and the cost function based on Huber

is reconstructed, which we propose a new filtering algorithm. In Section IV, the new algorithm is applied to the target tracking model for numerical analysis, and performance results are presented. Finally, the outcomes of the research are summarized in Section V.

II. UNSCENTED KALMAN FILTER

Standard UKF algorithms for nonlinear discrete systems is defined as:

$$\begin{cases} X_k = f_{k-1}(X_{k-1}) + w_{k-1} \\ Z_k = h_k(X_k) + v_k \end{cases} \quad (1)$$

where $X_k \in \mathbb{R}^n$ and $Z_k \in \mathbb{R}^m$ denote the state vector and measurement vector at a time step k , respectively, and with corresponding dimensions. $f(\cdot)$ and $h(\cdot)$ are any known functions, that denote nonlinear dynamic model function and measurement model function, respectively, and with corresponding dimensions. w_k is the process noise and v_k is the observation noise, respectively, and with uncorrelated Gaussian white-noise sequence. The following statistical characteristics are used:

$$\begin{cases} E[w_k] = 0 & cov(w_k, w_j) = \mathbf{Q}_k \delta_{kj} \\ E[v_k] = 0 & cov(v_k, v_j) = \mathbf{R}_k \delta_{kj} \\ cov(w_k, v_j) = 0 \end{cases} \quad (2)$$

where \mathbf{Q}_k and \mathbf{R}_k are positive definite matrices, with corresponding dimensions. δ_{kj} is Kronecker – δ function. The standard UKF filtering algorithm for nonlinear systems is as follows:

Initialization:

$$\begin{cases} \hat{X}_0 = E[X_0] \\ P_0 = E[(X_0 - \hat{X}_0)(X_0 - \hat{X}_0)^T] \end{cases} \quad (3)$$

Sigma point calculation:

$$\begin{cases} \xi_{k-1}^i = \hat{X}_{k-1}, & i = 0 \\ \xi_{k-1}^i = \hat{X}_{k-1} + (\sqrt{(n+\lambda)P_{k-1}})_i, & i = 1 \sim n \\ \xi_{k-1}^i = \hat{X}_{k-1} - (\sqrt{(n+\lambda)P_{k-1}})_i, & i = n+1 \sim 2n \end{cases} \quad (4)$$

$$\begin{cases} \omega_c^0 = \frac{\lambda}{n+\lambda} \\ \omega_m^0 = \frac{\lambda}{n+\lambda} + (1 - \alpha^2 + \beta) \\ \omega_c^i = \omega_m^i = \frac{\lambda}{2(n+\lambda)} \end{cases} \quad (5)$$

where $\lambda = \alpha^2(n + \kappa) - n$ is a scaling parameter that reduces the total prediction error. α , κ and n are the state control of sampling point distribution, parameters to be selected, and state dimension, respectively, with different models. α is usually set to $1e-4 \leq \alpha \leq 1$. i denotes the i th sampling point and $(\sqrt{(n+\lambda)P})_i$ denotes the column of the square root of the matrix $(n+\lambda)P$. $\beta \geq 0$ is a parameter that is to be selected and is a non-negative weight coefficient. $\beta \geq 0$ can combine the dynamic difference of the higher order in the equation.

Time update:

$$\xi_{k|k-1}^i = f(\xi_{k-1}^i), i = 0 \sim 2n \quad (6)$$

$$\hat{X}_{k|k-1} = \sum_{i=0}^{2n} \omega_m^i \xi_{k|k-1}^i \quad (7)$$

$$P_{k|k-1} = \sum_{i=0}^{2n} \omega_c^i (\xi_{k|k-1}^i - \hat{X}_{k|k-1}^i)(\xi_{k|k-1}^i - \hat{X}_{k|k-1}^i)^T + \mathbf{Q}_k \quad (8)$$

Measurement update:

$$\begin{cases} \xi_{k|k-1}^i = \hat{X}_{k|k-1}, & i = 0 \\ \xi_{k|k-1}^i = \hat{X}_{k|k-1} + (\sqrt{(n+\lambda)P_{k|k-1}})_i, & i = 1 \sim n \\ \xi_{k|k-1}^i = \hat{X}_{k|k-1} - (\sqrt{(n+\lambda)P_{k|k-1}})_i, & i = n+1 \sim 2n \end{cases} \quad (9)$$

$$\gamma_{k|k-1}^i = h(\xi_{k|k-1}^i) \quad (10)$$

$$\hat{Z}_{k|k-1} = \sum_{i=0}^{2n} \omega_m^i \gamma_{k|k-1}^i \quad (11)$$

$$P_{k|k-1}^{zz} = \sum_{i=0}^{2n} \omega_c^i (\gamma_{k|k-1}^i - \hat{Z}_{k|k-1})(\gamma_{k|k-1}^i - \hat{Z}_{k|k-1})^T + \mathbf{R}_k \quad (12)$$

$$P_{k|k-1}^{xz} = \sum_{i=0}^{2n} \omega_c^i (\xi_{k|k-1}^i - \hat{X}_{k|k-1}^i)(\gamma_{k|k-1}^i - \hat{Z}_{k|k-1})^T \quad (13)$$

$$K_k = P_{k|k-1}^{xz} (P_{k|k-1}^{zz})^{-1} \quad (14)$$

$$\hat{X}_{k|k} = \hat{X}_{k|k-1} + K_k (Z_k - \hat{Z}_{k|k-1}) \quad (15)$$

$$P_{k|k} = P_{k|k-1} - K_k P_{k|k-1}^{zz} K_k^T \quad (16)$$

III. A NEW ROBUST ADAPTIVE UKF ALGORITHM

A. SVD METHOD

The SVD is used to suppress the negative definiteness of the state covariance matrix of the system. To overcome the ill-conditioned matrix encountered by the UKF method in the calculation of the covariance, we used an SVD strategy to replace the inverse operation of covariance in the standard UKF gain matrix. The numerical sensitivity operation of matrix inversion is avoided, the computational complexity is reduced, and the robustness of the algorithm is further improved.

Lemma 1: $A \in R^{m \times n}$ ($m \geq n$), where A is an arbitrary symmetric positive definite matrix with corresponding dimensions. The SVD decomposition of a matrix can be expressed as: $A = U \Lambda V^T = U \begin{bmatrix} S & 0 \\ 0 & 0 \end{bmatrix} V^T$, which satisfies the conditions described below: $U \in R_{m \times n}$, $V \in R_{n \times n}$, $s_1 \geq s_2 \geq \dots \geq s_n$, $S = diag(s_1, s_2, \dots, s_n)$, where S is SVD of Matrix A with the decreasing order of values. U and V are left-singular vector and right-singular vector, respectively, with corresponding dimensions [58].

Proposition 1: Based on Lemma 1, if P is a symmetric positive definite matrix, the following values are obtained:

$$K_k = P_{k|k-1}^{xz} U_{k|k-1}^{zz} (D_{k|k-1}^{zz} D_{k|k-1}^{Tzz})^{-1} U_{k|k-1}^{Tzz} \quad (17)$$

$$P_{k|k} = [S_{k|k-1} \quad -K_k S_{k|k-1}^{zz}] [S_{k|k-1} \quad -K_k S_{k|k-1}^{zz}]^T \quad (18)$$

Details of the above certification process are given in Appendix A. By getting $S_{k|k} = [S_{k|k-1} \ - K_k S_{k|k-1}^{zz}]$ to QR calculation and entering to the next iteration, we introduce the QR detailed derivation of the method in the next section.

B. QR DECOMPOSITION METHOD

In UKF operation, we need to decompose the state covariance matrix by Cholesky. Because of the distribution of the UKF weight and sampling points, the covariance matrix P is non-positive definite or asymmetric after repeated cyclic updates. In this paper, QR decomposition is introduced to solve the non-positive definiteness problem of the covariance matrix in UKF filtering and effectively avoid the ill-conditioned filter numerical. The covariance is decomposed into orthogonal Matrix Q and upper triangular Matrix R by the QR method. The result of the QR decomposition is unique. Matrix Q has a strong ability to resist geometric attack, and Matrix R is an upper triangular matrix where the energy is concentrated. Therefore, it is feasible to process covariance data by the QR decomposition. The QR method improves the numerical stability of the filtering algorithm and reduces the state estimation error. Thus, the computational efficiency of state estimation can be improved in general.

Lemma 2: Let $A \in R^{m \times n}$ ($m \geq n$), $Q \in R^{m \times m}$ are unitary matrices with corresponding dimensions. $Q^T A = \begin{bmatrix} R \\ 0 \end{bmatrix}$, where R is the upper triangular matrix with $n \times$ dimensions. It is called the QR decomposition of A [59].

Proposition 2: Based on Lemma 2, if A is the square root of the P , decomposition of A is:

$$P_{k|k-1} = R_{k|k-1} R_{k|k-1}^T \quad (19)$$

$$P_{k|k} = R_{k|k} R_{k|k}^T \quad (20)$$

Details of the above certification process are given in Appendix B.

In order to overcome the ill-conditioned matrix of the covariance in the filtering process, we used the SVD strategy to replace the inverse operation in the gain matrix, and the property of QR decomposition is used to solve the non-positive definiteness of the covariance in the UKF algorithm. Through this derivation process, a new QS-UKF algorithm is helpful to improve the numerical stability and ensure the positive definiteness of covariance. We can save the computational complexity as much as possible and avoid any operation of generalized inverse in time-varying systems.

The implementation of the proposed QS-UKF algorithm is formulated as follows:

- 1) Initialization:

$$\hat{X}_0 = E[X_0] \quad P_0 = S_0 S_0^T \quad (21)$$

Time-update:

- 2) Skip the factorization of the state estimation error covariance matrix because the square root matrix $S_{k-1|k-1}$ is available, and start calculation from (4)-(7).

- 3) The square root of the covariance matrix of state one-step prediction error is calculated:

$$S_{k|k-1} = qr([\chi_{k|k-1} \ S_{Q,k-1}]) \quad (22)$$

where $qr(\cdot)$ denotes the proposition 2 proposed QR method and $\mathbf{Q}_{k-1} = S_{Q,k-1} S_{Q,k-1}^T$, and the weighted centered matrix is:

$$\begin{aligned} \chi_{k|k-1} &= \frac{\kappa}{\sqrt{2(n+\kappa)}} [\sqrt{2\kappa}(\xi_{k|k-1}^0 - \hat{X}_{k|k-1}) \\ &\quad \times \xi_{k|k-1}^1 - \hat{X}_{k|k-1} \cdots \xi_{k|k-1}^{2n} - \hat{X}_{k|k-1}] \end{aligned} \quad (23)$$

Measurement-update:

- 4) Skip the factorization of the state estimation error covariance matrix because the square root matrix $S_{k|k-1}$ is available, and start calculation from (10)-(11).

$$S_{zz,k|k-1} = qr([\zeta_{k|k-1} \ S_{Q,k-1}]) \quad (24)$$

where $R_{k-1} = S_{R,k-1} S_{R,k-1}^T$, $P_{zz,k|k-1} = S_{zz,k|k-1} S_{zz,k|k-1}^T$, and the weighted centered matrix is:

$$\begin{aligned} \zeta_{k|k-1} &= \frac{\kappa}{\sqrt{2(n+\kappa)}} [\sqrt{2\kappa}(\gamma_{k|k-1}^0 - \hat{Z}_{k|k-1}) \\ &\quad \times \gamma_{k|k-1}^1 - \hat{Z}_{k|k-1} \cdots \gamma_{k|k-1}^{2n} - \hat{Z}_{k|k-1}] \end{aligned} \quad (25)$$

- 5) Using the SVD method for autocorrelation covariance:

$$[U, D, V] = SVD(S_{zz,k|k-1}) \quad (26)$$

- 6) The gain matrix is obtained by using equation (86):

$$K_k = P_{k|k-1}^{xz} U_{k|k-1}^{zz} (D_{k|k-1}^{zz} D_{k|k-1}^{Tzz})^{-1} U_{k|k-1}^{Tzz} \quad (27)$$

- 7) Calculate state estimation and covariance matrix:

$$\hat{X}_{k|k} = \hat{X}_{k|k-1} + K_k (Z_k - \hat{Z}_{k|k-1}) \quad (28)$$

$$\begin{aligned} P_{k|k-1} &= [S_{k|k-1} - K_k S_{k|k-1}^{zz}] [S_{k|k-1} - K_k S_{k|k-1}^{zz}]^T \\ &= S_{k|k} S_{k|k}^T \end{aligned} \quad (29)$$

C. OPTIMAL ADAPTIVE FACTOR BASED ON NONLINEAR FILTERING

To enhance the robustness of the filter with respect to the uncertainty of the system model and the tracking ability of the system state mutation, we selected the optimal time-varying gain matrix K based on the idea of strong tracking. When the system reaches the stationary state, the gain matrix tends to be minimized; if the state changes suddenly, the prediction residuals increase, and the filter becomes divergent. In this case, the filter provides theoretical innovation covariance based on the predicted residual vector ε_k that mainly reflects the error of kinematics model information. In order to improve the tracking ability of system state mutation and to select optimal

time-varying gain matrix K , we introduced the following performance indicators:

$$E[x_k - \hat{x}_k][x_k - \hat{x}_k]^T = \min \quad (30)$$

$$E[\varepsilon_{k+j}\varepsilon_k^T] = 0 (k = 0, 1, 2, \dots; j = 1, 2, \dots) \quad (31)$$

The residual sequence can be expressed as:

$$\varepsilon_k = Z_k - \hat{Z}_{k|k-1} \quad (32)$$

Equations (30) and (31) indicate that the performance of the filter and the residual sequence required at different time points are always orthogonal to each other. However, in the actual system, because of the mismatch of the model, the state estimation of the filter deviates from the real value, resulting in the nonorthogonal output residual sequence. In order to maintain better tracking ability, we introduced the fading factor into the prediction of the state error covariance matrix to online adjust the error covariance and gain matrix. By enlarging the covariance matrix λ times, we increased the proportion of observed data in system state estimation. The forced residual sequence is still orthogonal to each other to guarantee the tracking ability of the filter. The adaptive fading factor λ_k is introduced to predict the covariance matrix $P_{k|k-1}$ and to improve the adaptability of the system.

$$P_{k|k-1} = \lambda_k \sum_{i=0}^{2n} \omega_c^i (\xi_{k|k-1}^i - \hat{X}_{k|k-1}^i) \times (\xi_{k|k-1}^i - \hat{X}_{k|k-1}^i)^T + \mathbf{Q}_k \quad (33)$$

The analytical solution of λ_k is given by the following: From the system equation and measurement equation, we know that:

$$\tilde{X}_k = X_k - \hat{X}_k \quad (34)$$

$$\tilde{X}_{k-1} = X_{k-1} - \hat{X}_{k-1} \quad (35)$$

$$\tilde{X}_{k|k-1} = X_k - \hat{X}_{k|k-1} = F_k \tilde{X}_{k-1} + w_{k-1} \quad (36)$$

where F_k refers to the Jacobian matrix $f(\cdot)$ and can be solved in the way of second-order moment or higher-order Taylor series expansion. It is calculated as follows [60]: $F_k = \frac{\partial f_k(X_k)}{\partial X_k} |_{X_k=\hat{X}_{k-1}}$. Defining innovation vector, we obtain:

$$\begin{aligned} \varepsilon_k &= Z_k - \hat{Z}_{k|k-1} = H_k \tilde{X}_{k|k-1} + v_k \\ &= H_k [F_k \tilde{X}_{k-1} + w_{k-1}] + v_k \end{aligned} \quad (37)$$

Without loss of generality:

$$\varepsilon_{k+j} = H_{k+j} [F_{k+j} \tilde{X}_{k+j-1} + w_{k+j-1}] + v_{k+j} \quad (38)$$

where H_k refers to the Jacobian matrix $h(\cdot)$ and can be solved in the way of the second-order moment or higher-order Taylor series expansion. It is calculated as follows [60]: $H_k = \frac{\partial h_k(X_k)}{\partial X_k} |_{X_k=\hat{X}_{k|k-1}}$.

$$\begin{aligned} P_{k|k-1}^{zz} &= E[Z_k - \hat{Z}_{k|k-1}][Z_k - \hat{Z}_{k|k-1}]^T \\ &= H_k P_{k|k-1} H_k^T + \mathbf{R}_k \end{aligned} \quad (39)$$

$$\begin{aligned} P_{k|k-1}^{xz} &= E[X_k - \hat{X}_{k|k-1}][Z_k - \hat{Z}_{k|k-1}]^T \\ &= P_{k|k-1} H_k^T \end{aligned} \quad (40)$$

$$\begin{aligned} \eta_{k,j} &= E[\varepsilon_{k+j}\varepsilon_k^T] \\ &= E[H_{k+j}(F_{k+j}\tilde{X}_{k+j-1} + w_{k+j-1}) + v_{k+j}] \\ &\quad \times [H_k(F_k\tilde{X}_{k-1} + w_{k-1}) + v_k]^T \\ &= H_{k+j} F_{k+j} \left(\prod_{i=k+1}^{k+j-1} (I - K_i H_i) F_i \right) (P_{k|k-1}^{xz} - K_k \eta_0) \end{aligned} \quad (41)$$

where η_0 is the innovation covariance matrix of the actual output of the filter. Let $\eta_{k,j} = 0$, then $(P_{k|k-1}^{xz} - K_k \eta_0) = 0$. Through calculation and arrangement:

$$P_{k|k-1}^{xz} (I - (P_{k|k-1}^{zz})^{-1} \eta_0) = 0 \quad (42)$$

$$P_{k|k-1} H_k^T (I - (H_k P_{k|k-1} H_k^T + R_k)^{-1} \eta_0) = 0 \quad (43)$$

$$H_k P_{k|k-1} H_k^T = \eta_0 - \mathbf{R}_k \quad (44)$$

Bring the modified covariance:

$$\begin{aligned} H_k \{ \lambda_k \sum_{i=0}^{2n} \omega_c^i (\xi_{k|k-1}^i - \hat{X}_{k|k-1}^i) \\ \times (\xi_{k|k-1}^i - \hat{X}_{k|k-1}^i)^T + \mathbf{Q}_k \} H_k^T = \eta_0 - \mathbf{R}_k \end{aligned} \quad (45)$$

$$\begin{aligned} H_k \lambda_k \sum_{i=0}^{2n} \omega_c^i (\xi_{k|k-1}^i - \hat{X}_{k|k-1}^i) (\xi_{k|k-1}^i - \hat{X}_{k|k-1}^i)^T H_k^T \\ = \eta_0 - \mathbf{R}_k - H_k \mathbf{Q}_k H_k^T \end{aligned} \quad (46)$$

$$\eta_k = \begin{cases} \varepsilon_1 \varepsilon_1^T, & k = 1 \\ \frac{\rho \eta_{k-1} + \varepsilon_k \varepsilon_k^T}{1 + \rho}, & k \geq 2 \end{cases} \quad (47)$$

where ρ is the softening factor, whose the value is 0.95.

$$\begin{aligned} \lambda_k &= \text{tr}(\eta_k - \mathbf{R}_k - H_k \mathbf{Q}_k H_k^T) / \text{tr}(H_k \sum_{i=0}^{2n} \omega_c^i \\ &\quad \times (\xi_{k|k-1}^i - \hat{X}_{k|k-1}^i) (\xi_{k|k-1}^i - \hat{X}_{k|k-1}^i)^T H_k^T) \end{aligned} \quad (48)$$

To guarantee the stability of the whole filtering process, we set the value of fading factor to greater than 1:

$$\lambda_k = \max(1, \lambda_k) \quad (49)$$

Based on the framework of UKF, the flow chart of the adaptive UKF algorithm is given in the Appendix C.

D. COST FUNCTION OF THE ROBUST NONLINEAR FILTERING METHOD

The objective of the proposed algorithm is to solve the state estimation problems caused by state mutation and measurement outliers. This work focuses on the issues of state mutation and measurement outliers. For the state space model (1), the combined cost function is used to make two different criteria for the state model and the measurement model. It is assumed that the state space model is

accurate in equation (1). From the Bayesian point of view, equation (1) can be solved according to the following cost functions using Bayesian maximum likelihood. The posterior mean estimation is obtained by minimizing the following cost functions:

$$\hat{X}_{k|k} = \arg \min(\|X_k - \hat{X}_{k|k-1}\|_{P_{k|k-1}}^2 + \|Z_k - h(X_k)\|_{R_k^{-1}}^2) \quad (50)$$

where $\|X\|_A^2 = X^T A X$, assuming A is the non-negative definite that denotes the quadratic form of A . $\hat{X}_{k|k}$ denotes posterior mean estimate. $\hat{X}_{k|k-1}$ and $P_{k|k-1}$ are the state prediction and correlation prediction covariance matrix, respectively.

To improve the robustness of traditional UKF to model error, the adaptive filtering algorithm proposed combined with the Huber filtering algorithm, and adaptive adjustment factor enhances the robustness of the model error. Rearrangement equation (50), we obtain:

$$\hat{X}_{k|k} = \arg \min(\|X_k - \hat{X}_{k|k-1}\|_{(\lambda_k P_{k|k-1})^{-1}}^2 + \sum_{j=1}^m \rho(\varepsilon_j)) \quad (51)$$

where λ_k is the adaptive adjustment factor, $\rho(\cdot)$ and m are the convex robust compensation function and dimension of the measurement model, respectively.

Suppose $\varepsilon_k = R_k^{-1/2}(Z_k - h(X_k))$, then, Huber introduces the following form of cost function:

$$\rho(\zeta) = \begin{cases} 0.5\zeta^2 & |\zeta| < r \\ r|\zeta| - 0.5r^2 & |\zeta| \geq r \end{cases} \quad (52)$$

where r is the tuning parameter that is typically set to 1.345, and ζ is the residual vector. Let $e_k = P_{k|k-1}^{-1/2}(X_k - \hat{X}_{k|k-1})$ denote modified robust cost function. Equation (51) is reorganized to get:

$$\hat{X}_{k|k} = \arg \min\left(\frac{1}{2}\lambda_k^{-1} \sum_{i=1}^n (e_{k,i})^2 + \sum_{j=1}^m \rho(\varepsilon_{k,j})\right) \quad (53)$$

where n denotes the dimension of the process model. $e_{k,i}$ and $\varepsilon_{k,j}$ are the i th component of e_k and the j th component of ε_k , respectively, with the moment k . To solve the minimization problem, we can derive equation (53) from the implicit equation as:

Let $\phi(\varepsilon_k) = \rho'(\varepsilon_k)$ be the influence function.

$$\lambda_k^{-1} \sum_{i=1}^n e_{k,i} \frac{\partial e_{k,i}}{\partial x_k} + \sum_{j=1}^m \phi(\varepsilon_{k,j}) \frac{\partial \varepsilon_{k,j}}{\partial x_k} = 0 \quad (54)$$

Defined $\psi(\varepsilon_{k,j}) = \phi(\varepsilon_{k,j})/\varepsilon_{k,j}$ is the weight function and weight matrix $\Psi = \text{diag}(\psi(\varepsilon_{k,j}))$. Huber method uses weighted matrix Ψ to reconstruct measurement information. Equation (54) can be rewritten as follows:

$$\lambda_k^{-1} (P_{k|k-1}^T)^{-1} e_k + H_k^T (R_k^T)^{-1/2} \Psi \varepsilon_k = 0 \quad (55)$$

where H_k refers to the Jacobian matrix $h(\cdot)$ and can be solved the second-order moment or higher-order Taylor series expansion.

The weight function expression is:

$$\psi(\varepsilon_{k,j}) = \begin{cases} 1 & |\varepsilon_{k,j}| < r \\ \text{sgn}(\varepsilon_{k,j})r/\varepsilon_{k,j} & |\varepsilon_{k,j}| \geq r \end{cases} \quad (56)$$

Substituting the denotation of e_k and ε_k into equation (55) yields,

$$(\lambda_k P_{k|k-1})^{-1}(X_k - \hat{X}_{k|k-1}) + H_k^T (R_k^T)^{-1/2} \Psi \times R_k^{-1/2}(Z_k - h(X_k)) = 0 \quad (57)$$

The revised covariance is defined as:

$$\tilde{P}_{k|k-1} = \lambda_k P_{k|k-1} \quad \tilde{R}_k = (R_k^T)^{1/2} \Psi^{-1} R_k^{1/2} \quad (58)$$

Then equation (57) can be rewritten as follows:

$$\hat{X}_{k|k} = \arg \min(\|X_k - \hat{X}_{k|k-1}\|_{\tilde{P}_{k|k-1}}^2 + \|Z_k - h(X_k)\|_{\tilde{R}_k^{-1}}^2) \quad (59)$$

In contrast to equations (59) and (50), it is easy to find the same structure, except that $\tilde{P}_{k|k-1}$ and \tilde{R}_k are different. If λ_k and Ψ set to identities, the improved adaptive robust filtering algorithm is reduced to a standard UKF. Therefore, to embed the modified covariance $\tilde{P}_{k|k-1}$ and \tilde{R}_k into the UKF framework is feasible without approximating the non-linear function.

A new adaptive robust UKF algorithm is determined as follows:

- 1) The initial value is given by equation (3) and applied to $X_0 = N(X_0; \bar{X}_0, P_0)$. Sigma point $\xi_{k-1}^{(i)\pm}$ and corresponding $\omega_{c/m}^i$ are calculated by equations (4) and (5).

Time update:

- 2) Evaluate the propagated sigma points:

$$\xi_{k|k-1}^i = f(\xi_{k-1}^{(i)\pm}) \quad (60)$$

- 3) Evaluate the predicted state:

$$\hat{X}_{k|k-1} = \sum_{i=0}^{2n} \omega_m^i \xi_{k|k-1}^i \quad (61)$$

- 4) The square root of the covariance matrix of state one-step prediction error is calculated:

$$S_{k|k-1} = qr([\chi_{k|k-1} \quad S_{Q,k-1}]) \quad (62)$$

- 5) The solution for $\chi_{k|k-1}$ is in equation (23).

- 6) The adaptive factor updated by equation (49):

$$\lambda_k = \max(1, \lambda_k) \quad (63)$$

- 7) Modified one-step predictive covariance:

$$\tilde{S}_{k|k-1} = \lambda_k S_{k|k-1} \quad (64)$$

Measurement update:

- 8) Sigma point $\xi_{k|k-1}^{(i)\pm}$ is calculated by equation (9).

9) Evaluate the propagated sigma points:

$$\gamma_{k|k-1}^i = h(\xi_{k|k-1}^{(i)\pm}) \quad (65)$$

10) Estimate the predicted measurement and the cross-covariance matrix:

$$\hat{Z}_{k|k-1} = \sum_{i=0}^{2n} \omega_m^i \gamma_{k|k-1}^i \quad (66)$$

$$P_{k|k-1}^{xz} = \sum_{i=0}^{2n} \omega_c^i (\xi_{k|k-1}^i - \hat{X}_{k|k-1}^i)(\gamma_{k|k-1}^i - \hat{Z}_{k|k-1})^T \quad (67)$$

11) Robust correction:

$$\varepsilon_k = \mathbf{R}_k^{-1/2}(Z_k - h(X_k)) \quad (68)$$

$$\psi(\varepsilon_{k,j}) = \begin{cases} 1 & |\varepsilon_{k,j}| < r \\ sgn(\varepsilon_{k,j})r/\varepsilon_{k,j} & |\varepsilon_{k,j}| \geq r \end{cases} \quad (69)$$

$$\Psi = diag(\psi(\varepsilon_{k,j})), j = 1, 2, \dots, m \quad (70)$$

$$\tilde{R} = (\mathbf{R}_k^T)^{1/2} \Psi^{-1} \mathbf{R}_k^{1/2} \quad (71)$$

12) The square root matrix of the covariance matrix of measurement $S_{k|k-1}$:

$$S_{zz,k|k-1} = qr([\zeta_{k|k-1} \quad S_{\tilde{R},k-1}]) \quad (72)$$

13) The solution for $\zeta_{k|k-1}$ is in equation (25).

$$[U, D, V] = SVD(S_{zz,k|k-1}) \quad (73)$$

14) Finally, estimate the updated state, the Kalman gain and the corresponding error covariance:

$$K_k = P_{k|k-1}^{xz} U_{k|k-1}^{zz} (D_{k|k-1}^{zz} D_{k|k-1}^{Tzz})^{-1} U_{k|k-1}^{Tzz} \quad (74)$$

$$\hat{X}_{k|k} = \hat{X}_{k|k-1} + K_k(Z_k - \hat{Z}_{k|k-1}) \quad (75)$$

$$P_{k|k} = [S_{k|k-1} \quad -K_k S_{k|k-1}^{zz}] \times [S_{k|k-1} \quad -K_k S_{k|k-1}^{zz}]^T \quad (76)$$

IV. NUMERICAL STUDY

This section outlines several numerical test cases using the target tracking model to verify our proposed QS-ARUKF. Passive radar target tracking usually faces the data processing problems of strong nonlinearity and high speed measurement. In this paper, the two-dimensional nonlinear of bearings-only-tracking (BOT) model, which is consistent with [61] and [62], is chosen as the basis for the verification of the new algorithm proposed in this paper. The discrete model is obtained as follows:

$$\begin{cases} X_k = \begin{bmatrix} 0.9 & 0 \\ 0 & 1 \end{bmatrix} X_{k-1} + w_{k-1} \\ [0.5pc] Z_k = \tan^{-1} \left[\frac{X_{2,k} - \sin(k)}{X_{1,k} - \cos(k)} \right] + v_k \end{cases} \quad (77)$$

where $X_k = [X_{1,k} \ X_{2,k}]^T$ denotes the position of the Cartesian coordinate system. The sensor is an angle observer and its coordinate value is $(\cos(k), \sin(k))$ at k moment. w_k and

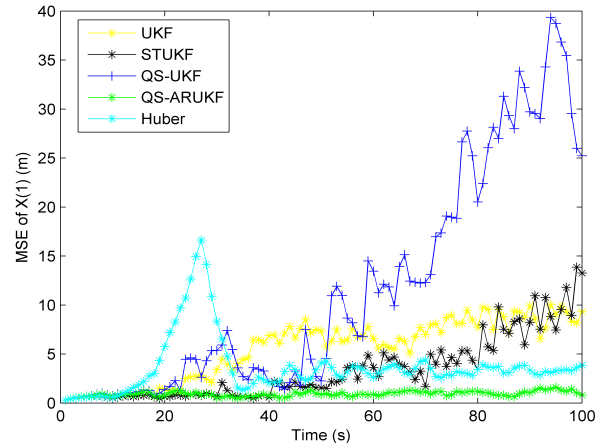


FIGURE 1. Mean square error of position state $X(1)$.

v_k are process noise and observation noise vectors, respectively, with zero mean Gaussian noise \mathbf{Q}_k and \mathbf{R}_k , and $k = 0, 1, \dots, M$, $M = 100$ runs 100 steps. The filter initial value is set to $X_0 = [20 \ 5]^T$, $P_0 = [0.1 \ 0; 0 \ 0.1]$, $w_k = N(0, \mathbf{Q}_k)$, $\mathbf{Q}_k = [0.1 \ 0.05; 0.05 \ 0.1]$, $v_k = (0, \mathbf{R}_k)$, and $\mathbf{R}_k = 0.025$. In the process of simulation, the Mean Square Error (MSE) that is used as the technical index to evaluate the filtering performance is defined as follows:

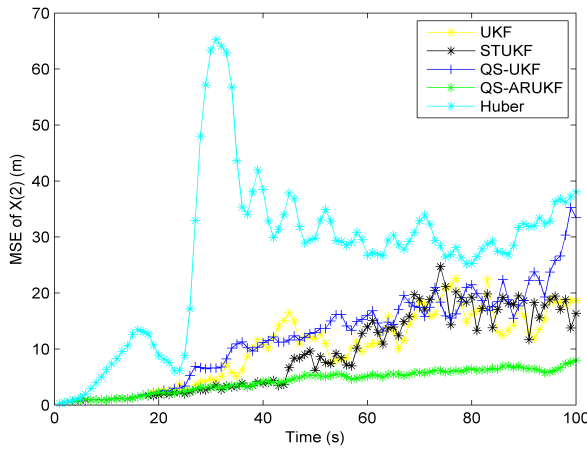
$$MSE_k = \frac{1}{N} \sum_{k=1}^N (X_k - X_{k|k})^2, \quad k = 1, 2, \dots, M \quad (78)$$

where N is 100 and denotes the number of Monte Carlo simulations, and the radar sampling period is 1 s. The simulation results are as follows:

A. CASE 1: RANDOM INITIAL ERROR

To verify the filtering accuracy of the algorithm under strongly nonlinear conditions, we added random initial error to Case 1. Initial error obeys $\hat{X}_0 \sim N(\hat{X}_0; X_0, P_0)$, and the test experiment is carried out without adding any large disturbance information. The simulation results are shown in Figs. 1 and 2, and Table 1 shows the numerical results of mean MSE. Where the UKF represents the standard Unscented Kalman Filter algorithm; STUKF represents the UKF algorithm derived from the principle of orthogonality; QS-UKF represents the UKF algorithm derived from the QR and SVD methods; Huber represents the UKF algorithm derived from the Huber cost function; QS-ARUKF represents the method proposed in this paper.

Fig. 1 shows that the tracking performance of the UKF, QS-UKF, and Huber algorithm is poor after 24 s in the strong nonlinear model. However, the tracking performance of the Huber method is better than that of those filtering methods after 34 s, and the error is still higher than that of the algorithm proposed in this paper. Although STUKF has no relatively large fluctuation, the error is also higher than the algorithm proposed in this paper. In Fig. 2, Huber has the largest error after 24 s, while the error curves of

**FIGURE 2.** Mean square error of position state $X(2)$.**TABLE 1.** The mean MSE of different algorithms.

Algorithm	$X(1)$	$X(2)$	Single step running time
UKF	5.439339	9.911633	0.000352
STUKF	3.315328	9.105420	0.000459
QS-UKF	11.482834	12.129102	0.001232
Huber	3.647203	26.727478	0.000134
QS-ARUKF	0.914617	4.248836	0.001287

TABLE 2. The mean MSE of different algorithms.

Algorithm	$X(1)$	$X(2)$	Single step running time
UKF	3.490847	26.772239	0.000371
STUKF	2.530379	15.956303	0.000482
QS-UKF	16.856988	29.270778	0.001307
Huber	3.598859	49.331588	0.000141
QS-ARUKF	0.829320	13.455494	0.001359

STUKF, UKF, and QS-UKF increase slowly. Compared with other filtering algorithms, the error of the proposed algorithm in this paper is lower. Table 1 indicates that the proposed algorithm is superior to other filtering algorithms.

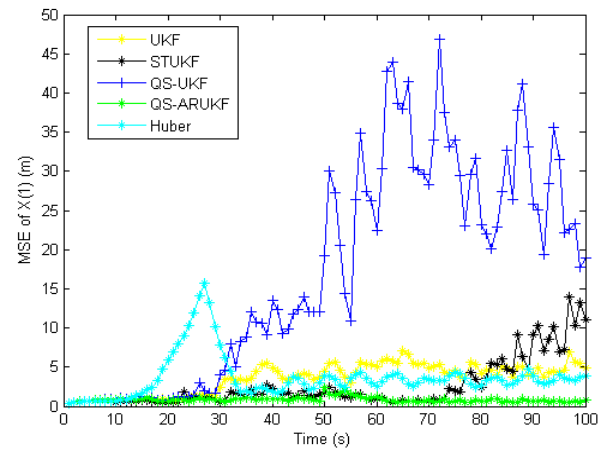
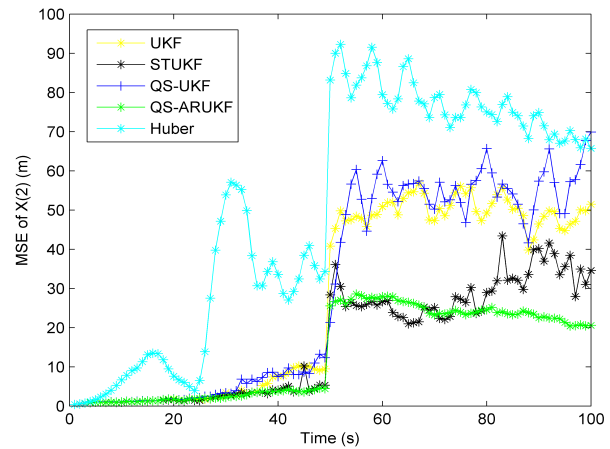
B. CASE 2: MODEL MISMATCH

In Case 2, to prove the superiority of the proposed algorithm and give the different disturbance information, we provide system model mismatch and measurement outlier as well as the coexistence of two situations.

1) SYSTEM MODEL MISMATCH

In this scenario, the perturbed information was superimposed under case 1, and a system model mismatch $\Delta X = [1 \ 5]^T$ was introduced at epochs of 50 s. The simulation results are shown in Figs. 3 and 4 and as well as Table 2.

In Fig. 3, the QS-UKF method deviated from the real trajectory after 24 s. Compared with the UKF method, the Huber algorithm had a large mutation at 24 s, the accuracy was lower than that of UKF, and the error was larger than the STUKF method. The algorithm proposed in this paper remained stationary without large error in the case of state mutation. In Fig. 4, all filters have huge fluctuations at epochs of 50 s,

**FIGURE 3.** Mean square error of position state $X(1)$.**FIGURE 4.** Mean square error of position state $X(2)$.

Huber algorithm is the most obvious, and the error of UKF and QS-UKF is almost the same. The error of STUKF is slightly higher than that of the algorithm proposed in this paper. The results show that the proposed algorithm can effectively resist the influence of the process model parameters mismatched filtering solution and improve the estimation accuracy of classical UKF.

2) MEASUREMENT OUTLIER

In this scenario, the perturbed information was superimposed under Case 1, and a measurement outlier and consecutive measurement outliers were introduced at epochs of 50 s and 70 s to 75 s with $\Delta Z = -5$, respectively. The simulation results are shown in Figs. 5 and 6 as well as Table 3.

3) SYSTEM MODEL MISMATCH AND MEASUREMENT OUTLIER OCCUR SIMULTANEOUSLY

In this scenario, system model mismatch and measurement outlier are simultaneously superimposed under Case 1. The simulation results are shown in Figs. 7 and 8 as well as Table 4.

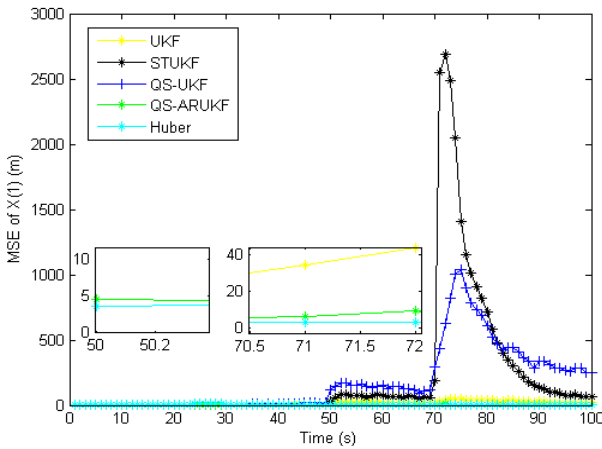
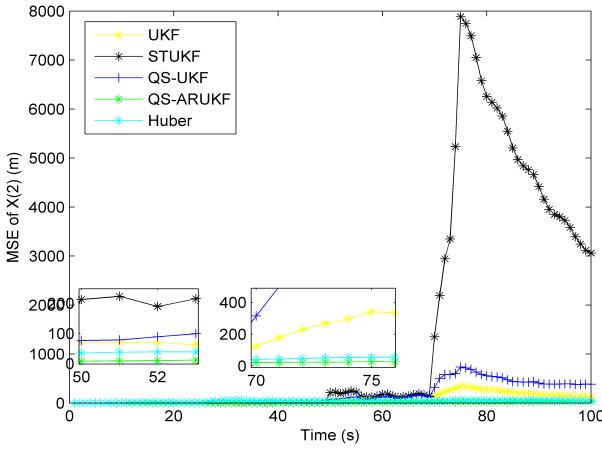
FIGURE 5. Mean square error of position state $X(1)$.FIGURE 6. Mean square error of position state $X(2)$.

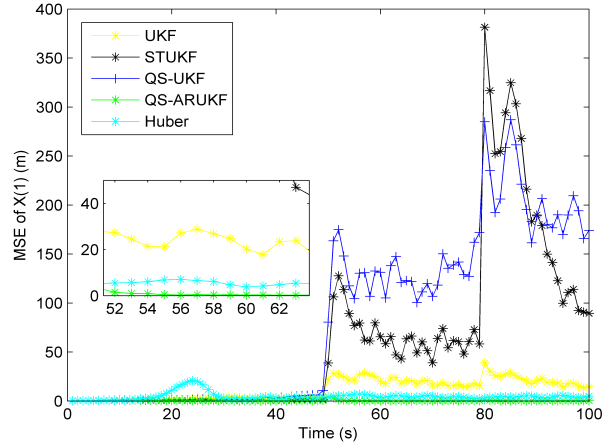
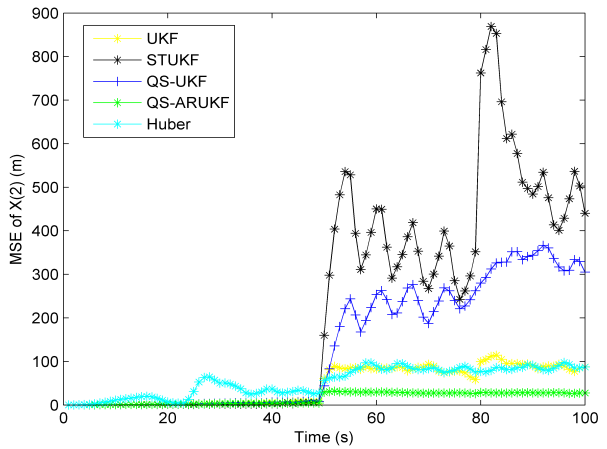
TABLE 3. The mean MSE of different algorithms.

Algorithm	$X(1)$	$X(2)$	Single step running time
UKF	17.377324	47.158156	0.000365
STUKF	115.67516	701.766976	0.000474
QS-UKF	121.35892	113.301424	0.001298
Huber	3.573317	33.070528	0.000139
QS-ARUKF	0.622881	6.041195	0.001343

TABLE 4. The mean MSE of different algorithms.

Algorithm	$X(1)$	$X(2)$	Single step running time
UKF	11.713758	45.032084	0.000356
STUKF	61.40466	225.182005	0.000460
QS-UKF	82.599248	134.205074	0.001283
Huber	4.733354	53.310374	0.000136
QS-ARUKF	0.56806	15.606986	0.001335

From Figs. 5 and 7, under the interference of measurement anomaly, except for the Huber method and QS-ARUKF algorithm proposed in this paper, all the other algorithms have abrupt changes of different sizes. Compared with the algorithm proposed in this paper, the Huber method has no large numerical fluctuation because Huber has a particular

FIGURE 7. Mean square error of position state $X(1)$.FIGURE 8. Mean square error of position state $X(2)$.

ability to deal with the uncertainty of the measurement model, but the error is still higher than that of the QS-ARUKF algorithm. It is clear from Figs. 6 and 8 that Huber and QS-ARUKF would fluctuate minimally when strong nonlinear state mutation and measurement anomaly coexist. However, QS-ARUKF is still superior to Huber algorithm because QS-ARUKF can effectively deal with the uncertainty of the system model and measurement model. The results show the superiority of the proposed algorithm under the condition of adding interference information.

C. CASE 3 SIMULATION ANALYSIS FOR UNKNOWN BOUNDED-NOISE INTERFERENCE

In practical applications, due to the inaccuracy of statistical characteristics of noise, Gaussian noise mixed with a small number of non-Gaussian noises. To further verify that the proposed algorithm is superior to other filtering algorithms, we carried out the following simulation analysis for the non-Gaussian state. Like the model mismatch, the performance of the proposed QS-ARUKF algorithm is evaluated from the

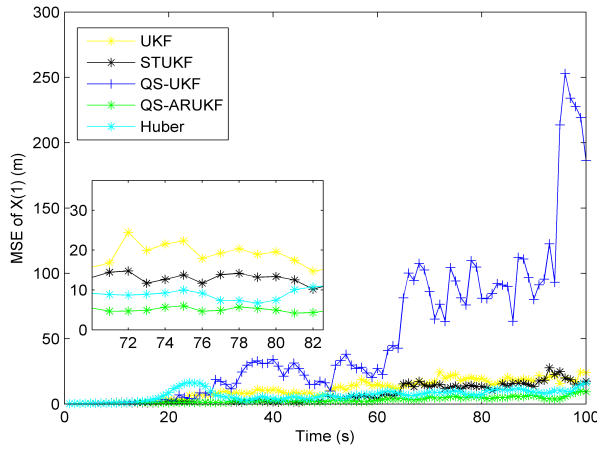


FIGURE 9. Mean square error of position state $X(1)$ with heavy-tailed process noise.

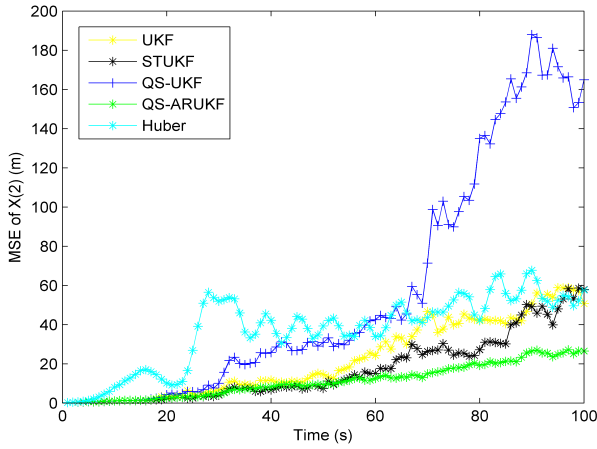


FIGURE 10. Mean square error of position state $X(2)$ with heavy-tailed process noise.

perspective of system noise, measurement noise, and mixed noise.

1) HEAVY-TAILED PROCESS NOISE

In this scenario, the heavy-tailed process noise was superimposed under the condition of Case 1. Outlier corrupted process noise was generated according to:

$$w_k \sim \begin{cases} N(0, \mathbf{Q}) & \text{w.p. 0.95} \\ N(0, 1.5\mathbf{Q}) & \text{w.p. 0.05} \end{cases} \quad (79)$$

where **w.p.** denotes "with probability". Definition equation (79) indicates that 5% of the process noise is generated by the Gaussian distribution with variance $1.5\mathbf{Q}$, and 95% of the process noise is generated by the Gaussian distribution with variance \mathbf{Q} . According to equation (79), the process noise has a heavy tail. The simulation results are shown in Figs. 9 and 10 as well as Table 5.

TABLE 5. The mean MSE of different algorithms with heavy-tailed process noise.

Algorithm	$X(1)$	$X(2)$	Single step running time
UKF	11.079755	22.237124	0.000377
STUKF	7.004802	16.935352	0.000494
QS-UKF	50.199029	56.545796	0.001334
Huber	6.914496	36.940636	0.000144
QS-ARUKF	2.987922	11.172409	0.001385

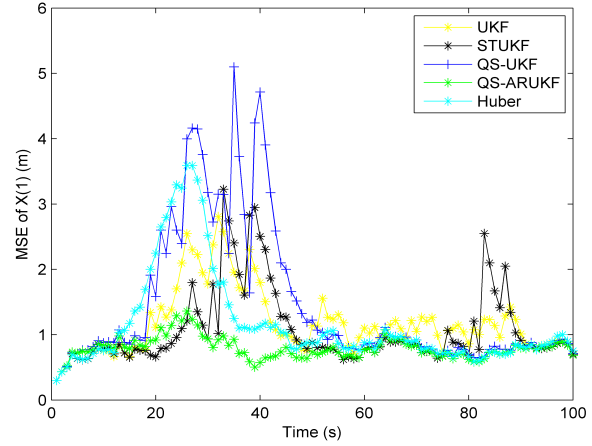


FIGURE 11. Mean square error of position state $X(1)$ with heavy-tailed measurement noise.

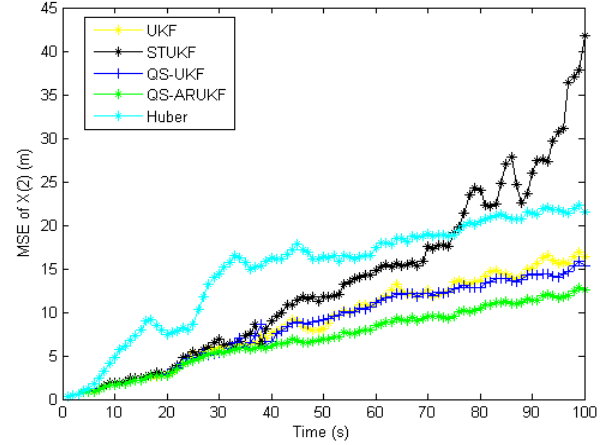


FIGURE 12. Mean square error of position state $X(2)$ with heavy-tailed measurement noise.

2) HEAVY-TAILED MEASUREMENT NOISE

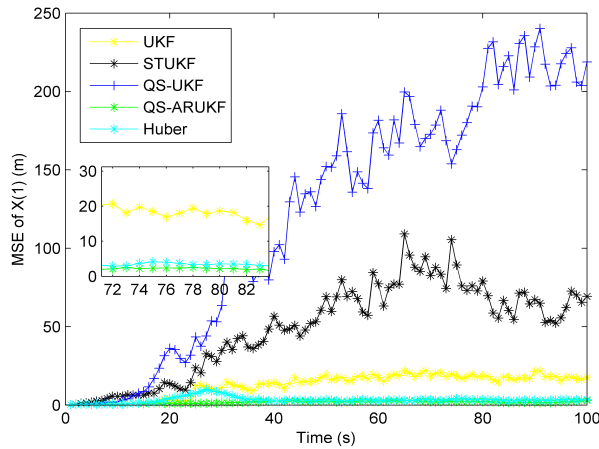
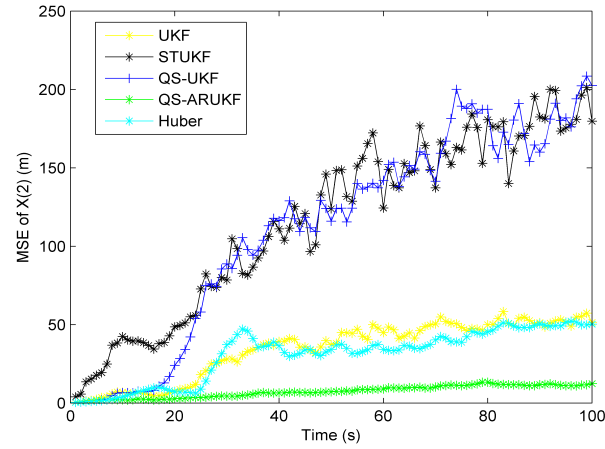
In this scenario, the heavy-tailed measurement noise was superimposed under Case 1. Outlier corrupted measurement noise was generated according to:

$$v_k \sim \begin{cases} N(0, \mathbf{R}) & \text{w.p. 0.95} \\ N(0, 100\mathbf{R}) & \text{w.p. 0.05} \end{cases} \quad (80)$$

The specific meaning is the same as equation (79). The simulation results are shown in Figs. 11 and 12 as well as Table 6.

TABLE 6. The mean MSE of different algorithms with heavy-tailed measurement noise.

Algorithm	X(1)	X(2)	Single step running time
UKF	1.165151	8.805746	0.000354
STUKF	1.061214	13.214514	0.000463
QS-UKF	1.444697	8.541751	0.001250
Huber	1.142113	14.791255	0.000136
QS-ARUKF	0.782374	6.929335	0.001300

**FIGURE 13.** Mean square error of position state X(1) with mixed Gaussian noise.**FIGURE 14.** Mean square error of position state X(2) with mixed Gaussian noise.

3) MIXED GAUSSIAN MODEL

In this scenario, the mixed Gaussian measurement noise was superimposed under Case 1. Outlier corrupted measurement noise are generated according to:

$$p(v) = (1 - \varepsilon)N(1, R_1) + \varepsilon N(0, \mathbf{R}) \quad (81)$$

where $p(\cdot)$ and $\varepsilon \in (0, 1)$ denote the probability density function and flashing probability, respectively. The variance of R_1 is greater than that of \mathbf{R} , and $\varepsilon = 0.5$, $R_1 = 1$. The simulation results are shown in Figs. 13 and 14 as well as Table 7.

TABLE 7. The mean MSE of different algorithms with mixed Gaussian noise.

Algorithm	X(1)	X(2)	Single step running time
UKF	12.709958	34.016164	0.000374
STUKF	48.421632	115.680247	0.000496
QS-UKF	121.441644	110.630078	0.001334
Huber	3.292347	30.700939	0.000143
QS-ARUKF	1.824505	7.216041	0.001393

In the BOT model of target tracking, the noise pollution is caused by deviating from the Gauss distribution; thus, state estimation will suffer from severe degradation. By introducing an adaptive factor, the influence of non-Gaussian noise on the system model uncertainty was adjusted. Also the modified covariance matrix was introduced into the Huber-M estimation framework. The Huber cost function has l_2 norm property of small residuals to ensure high efficiency with normal Gaussian distribution and has the l_1 norm for large residuals to suppress the effects of outliers and heavy-tailed non-Gaussian noise. The measurement information in the newly defined filtering framework is provided with good robustness for deviating from Gaussian behavior.

The MSEs from the proposed filter and existing filters are respectively shown in Figs. 9-14 as well as Tables 5-7. The error of the QS-ARUKF algorithm is smaller than that of other filters under the interference of process heavy tail, measurement heavy tail, and mixed Gaussian model. In particular, Fig. 11 shows that under the heavy-tailed measurement, all filters have different degrees of biased, but the error of the algorithm proposed in this paper is relatively stable. The proposed algorithm is also effective in non-Gaussian systems, and its accuracy is higher than other filters.

Tables 1-7 show that the algorithm proposed in this paper takes the longest time. However, it still satisfies the engineering requirements and fully proves that it is desirable to compromise time for accuracy.

V. CONCLUSION

In this paper, a new adaptive robust filtering algorithm for target tracking using the UKF formulation is derived. In the proposed algorithms, the Huber-M estimation method is used to suppress the anomaly of the measurement model, and the adaptive factor is derived to deal with the effect of dynamic model mismatch. The validity of matrix decomposition is guaranteed by QR decomposition in time update and measurement update, and the efficiency of state estimation is improved. The SVD method is used to avoid the matrix numerical sensitivity and to replace the matrix inversion. This method reduces the computational complexity and further improves the stability of the algorithm. The filter which satisfies the engineering requirements is easy to be realized. It has better filtering performance in the simulated cases of outliers. The comparison results show that the proposed algorithm is robust and stable under strong nonlinearity, state mutation, measurement outliers, and non-Gaussian noise.

APPENDIX A

DERIVATION OF PROPOSITION 1

Proof: Based on Lemma 1, if P is a symmetric positive definite matrix, the following values are obtained:

$$S_{k|k-1}^{zz} = U_{k|k-1}^{zz} D_{k|k-1}^{zz} V_{k|k-1}^{Tzz} \quad (82)$$

$$S_{k|k-1}^{Tzz} = (U_{k|k-1}^{zz} D_{k|k-1}^{zz} V_{k|k-1}^{Tzz})^T \quad (83)$$

In the upper form, $S_{k|k-1}^{zz}$ and $S_{k|k-1}^{Tzz}$ are represented by the SVD operation.

$$\begin{aligned} P_{k|k-1}^{zz} &= S_{k|k-1}^{zz} S_{k|k-1}^{Tzz} \\ &= (U_{k|k-1}^{zz} D_{k|k-1}^{zz} V_{k|k-1}^{Tzz})(U_{k|k-1}^{zz} D_{k|k-1}^{zz} V_{k|k-1}^{Tzz})^T \end{aligned} \quad (84)$$

$$(P_{k|k-1}^{zz})^{-1} = U_{k|k-1}^{zz} (D_{k|k-1}^{zz} D_{k|k-1}^{Tzz})^{-1} U_{k|k-1}^{Tzz} \quad (85)$$

$$\begin{aligned} K_k &= P_{k|k-1}^{xy} (P_{k|k-1}^{zz})^{-1} \\ &= P_{k|k-1}^{xy} U_{k|k-1}^{zz} (D_{k|k-1}^{zz} D_{k|k-1}^{Tzz})^{-1} U_{k|k-1}^{Tzz} \end{aligned} \quad (86)$$

$$\begin{aligned} P_{k|k} &= P_{k|k-1} - K_k P_{k|k-1}^{zz} K_k^T \\ &= S_{k|k-1} S_{k|k-1}^T - K_k S_{k|k-1}^{zz} (K_k^T S_{k|k-1}^{zz})^T \\ &= [S_{k|k-1} - K_k S_{k|k-1}^{zz}] [S_{k|k-1} - K_k S_{k|k-1}^{zz}]^T \\ &= S_{k|k} S_{k|k}^T \end{aligned} \quad (87)$$

APPENDIX B

DERIVATION OF PROPOSITION 2

Proof: If matrix $A_{k|k-1}$ is the square root of the matrix $P_{k|k-1}$, Cholesky operation is performed:

$$P_{k|k-1} = A_{k|k-1} A_{k|k-1}^T \quad (88)$$

$A_{k|k-1}$ is decomposed by QR :

$$\begin{aligned} A_{k|k-1} &= (Q_{k|k-1} R_{k|k-1})^T \\ A_{k|k-1}^T &= Q_{k|k-1} R_{k|k-1} \end{aligned} \quad (89)$$

where R and Q are the upper triangular matrix and unitary matrix, respectively, with corresponding dimensions.

$$\begin{aligned} P_{k|k-1} &= A_{k|k-1} A_{k|k-1}^T \\ &= (Q_{k|k-1} R_{k|k-1})^T (Q_{k|k-1} R_{k|k-1}) \\ &= R_{k|k-1}^T Q_{k|k-1}^T Q_{k|k-1} R_{k|k-1} \\ &= R_{k|k-1}^T R_{k|k-1} \end{aligned} \quad (90)$$

Without loss of generality:

$$P_{k|k} = R_{k|k}^T R_{k|k} \quad (91)$$

The above deduction proves the validity of equations (19) and (20).

APPENDIX C

STUKF ALGORITHM FLOW CHART

The flow chart of adaptive UKF algorithm is shown in Fig. 15.

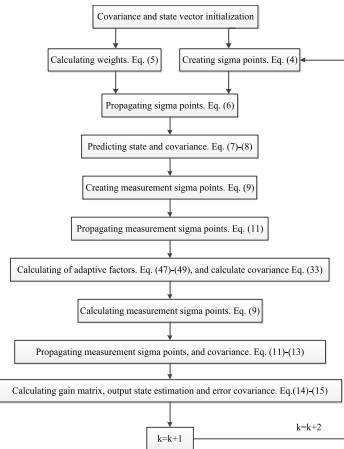


FIGURE 15. STUKF algorithm flow chart.

ACKNOWLEDGMENT

The authors would like to thank the editors and reviewers for their valuable comments on this paper.

REFERENCES

- [1] Y. Meng, S. Gao, Y. Zhong, G. Hu, and A. Subic, “Covariance matching based adaptive unscented Kalman filter for direct filtering in INS/GNSS integration,” *Acta Astron.*, vol. 120, pp. 171–181, Mar. 2016.
- [2] B. Allotta, A. Caiti, L. Chisci, R. Costanzo, F. Di Corato, C. Fantacci, D. Fenucci, E. Meli, and A. Ridolfi, “An unscented Kalman filter based navigation algorithm for autonomous underwater vehicles,” *Mechatronics*, vol. 39, pp. 185–195, Nov. 2016.
- [3] B. Allotta, A. Caiti, R. Costanzo, F. Fanelli, D. Fenucci, E. Meli, and A. Ridolfi, “A new AUV navigation system exploiting unscented Kalman filter,” *Ocean Eng.*, vol. 113, pp. 121–132, Feb. 2016.
- [4] B. Gao, G. Hu, S. Gao, Y. Zhong, and C. Gu, “Multi-sensor optimal data fusion for INS/GNSS/CNS integration based on unscented Kalman filter,” *Int. J. Control Autom. Syst.*, vol. 16, no. 1, pp. 129–140, Feb. 2018.
- [5] B. Gao, G. Hu, S. Gao, Y. Zhong, and C. Gu, “Multi-sensor optimal data fusion based on the adaptive fading unscented Kalman filter,” *Sensors*, vol. 18, no. 2, p. 488, Feb. 2018.
- [6] G. Hu, W. Wang, Y. Zhong, B. Gao, and C. Gu, “A new direct filtering approach to INS/GNSS integration,” *Aerospace Sci. Technol.*, vol. 77, pp. 755–764, Jun. 2018.
- [7] B. Gao, S. Gao, Y. Zhong, G. Hu, and C. Gu, “Interacting multiple model estimation-based adaptive robust unscented Kalman filter,” *Int. J. Control. Autom. Syst.*, vol. 15, no. 5, pp. 2013–2025, 2017.
- [8] F. Kumru, T. Akça, and E. Altuntas, “Ballistic target tracking using multiple model Kalman filter with *a priori* ballistic information,” in *Proc. 25th Signal Process. Commun. Appl. Conf. (SIU)*, Antalya, Turkey, May 2017, pp. 1–4.
- [9] Y. Yu, “Consensus-based distributed mixture Kalman filter for maneuvering target tracking in wireless sensor networks,” *IEEE Trans. Veh. Technol.*, vol. 65, no. 10, pp. 8669–8681, Oct. 2016.
- [10] Y. Tao, H. Geng, and P. Mehta, “Joint probabilistic data association-feedback particle filter for multiple target tracking applications,” in *Proc. Amer. Control Conf. (ACC)*, Montreal, QC, Canada, Jun. 2012, pp. 820–826.
- [11] Y. Cui, Z. Bo, W. Yang, Z. Wang, Y. Li, X. Yi, and Y. Tang, “End-to-end visual target tracking in multi-robot systems based on deep convolutional neural network,” in *Proc. IEEE Int. Conf. Comput. Vis. Workshops (ICCVW)*, Venice, Italy, Oct. 2017, pp. 1113–1121.
- [12] Y. Kim, W. Jung, and H. Bang, “Visual target tracking and relative navigation for unmanned aerial vehicles in a GPS-denied environment,” *Int. J. Aeronautical Space Sci.*, vol. 15, no. 3, pp. 112–121, Sep. 2014.
- [13] X. Wang, N. Cui, and J. Guo, “Huber-based unscented filtering and its application to vision-based relative navigation,” *IET Radar Sonar Navigat.*, vol. 4, no. 1, pp. 134–141, Feb. 2010.

- [14] F. Sun, X. Hu, Z. Yuan, and S. Li, "Adaptive unscented Kalman filtering for state of charge estimation of a lithium-ion battery for electric vehicles," *Energy*, vol. 36, no. 5, pp. 3531–3540, May 2014.
- [15] R. Xiong, F. Sun, Z. Chen, and H. He, "A data-driven multi-scale extended Kalman filtering based parameter and state estimation approach of lithium-ion olymer battery in electric vehicles," *Appl. Energy*, vol. 113, pp. 463–476, Jan. 2014.
- [16] B. M. Åkesson, J. B. Jørgensen, N. K. Poulsen, and S. B. Jørgensen, "A generalized autocovariance least-squares method for Kalman filter tuning," *J. Process Control*, vol. 18, no. 7, pp. 769–779, Aug./Sep. 2008.
- [17] M. F. Abdel-Hafez, "The autocovariance least-squares technique for GPS measurement noise estimation," *IEEE Trans. Veh. Technol.*, vol. 59, no. 2, pp. 574–588, Feb. 2010.
- [18] L. Chang, B. Hu, and G. Chang, "A robust single GPS navigation and positioning algorithm based on strong tracking filtering," *IEEE Sensors J.*, vol. 18, no. 0, pp. 290–298, Jan. 2017.
- [19] Y. Fan, Y. Zhang, G. Wang, X. Wang, and N. Li, "Maximum correntropy based unscented particle filter for cooperative navigation with heavy-tailed measurement noises," *Sensors*, vol. 18, no. 10, p. 3183, Oct. 2018.
- [20] Y. Huang and Y. Zhang, "A new process uncertainty robust Student's t based Kalman filter for SINS/GPS integration," *IEEE Access*, vol. 5, pp. 14391–14404, 2017.
- [21] Y. Huang, Y. Zhang, N. Li, and J. Chambers, "A robust Gaussian approximate fixed-interval smoother for nonlinear systems with heavy-tailed process and measurement noises," *IEEE Signal Process. Lett.*, vol. 23, no. 4, pp. 468–472, Apr. 2016.
- [22] Y. Huang, Y. Zhang, N. Li, S. M. Naqvi, and J. Chambers, "A robust student's t based cubature filter," in *Proc. 19th Int. Conf. Inf. Fusion (FUSION)*, Heidelberg, Germany, Jul. 2016, pp. 9–16.
- [23] P. J. Costa and W. H. Moore, "Extended Kalman-Bucy filters for radar tracking and identification," in *Proc. IEEE Nat. Radar Conf.*, Los Angeles, CA, USA, Mar. 1991, pp. 127–131.
- [24] G. Hu, S. Gao, and Y. Zhong, "A derivative UKF for tightly coupled INS/GPS integrated navigation," *ISA Trans.*, vol. 56, pp. 135–144, May 2015.
- [25] X. Wang, Q. Pan, Z. Ding, and Z. Ma, "Simultaneous mean and covariance correction filter for orbit estimation," *sensors*, vol. 18, no. 5, p. 1444, May 2018.
- [26] S. J. Julier and J. K. Uhlmann, "Unscented filtering and nonlinear estimation," *Proc. IEEE*, vol. 92, no. 3, pp. 401–422, Mar. 2004.
- [27] K. Xiong, H. Y. Zhang, and C. Chan, "Performance evaluation of UKF-based nonlinear filtering," *Automatica*, vol. 42, no. 2, pp. 261–270, 2006.
- [28] Y. Wu, D. Hu, and X. Hu, "Comments on "performance evaluation of UKF-based nonlinear filtering,'" *Automatica*, vol. 43, no. 3, pp. 567–568, Mar. 2017.
- [29] G. Wang, N. Li, and Y. Zhang, "Maximum correntropy unscented Kalman and information filters for non-Gaussian measurement noise," *J. Franklin Inst.*, vol. 354, no. 18, pp. 8659–8677, Dec. 2017.
- [30] X. Xie and G. Dai, "Unscented information filtering phase unwrapping algorithm for interferometric fringe patterns," *Appl. Opt.*, vol. 56, no. 34, pp. 9423–9434, Dec. 2017.
- [31] R. Xiong, Q. Yu, L. Y. Wang, and C. Lin, "A novel method to obtain the open circuit voltage for the state of charge of lithium ion batteries in electric vehicles by using H infinity filter," *Appl. Energy*, vol. 207, pp. 346–353, May 2017.
- [32] W. Li and Y. Jia, "H-infinity filtering for a class of nonlinear discrete-time systems based on unscented transform," *Signal Process.*, vol. 90, no. 12, pp. 3301–3307, Dec. 2010.
- [33] Q. Q. Yu, R. Xiong, C. Lin, W. X. Shen, and J. J. Deng, "Lithium-ion battery parameters and state-of-charge joint estimation based on H-infinity and unscented Kalman filters," *IEEE Trans. Veh. Technol.*, vol. 66, no. 10, pp. 8693–8701, Oct. 2017.
- [34] S. Ishihara and M. Yamakita, "Adaptive robust UKF for nonlinear systems with parameter uncertainties," in *Proc. 42nd Annu. Conf. IEEE Ind. Electron. Soc.*, Florence, Italy, Oct. 2016, pp. 48–53.
- [35] M. O. Karslioglu, E. Erdogan, and O. Pamuk, "GPS-based real-time orbit determination of low earth orbit satellites using robust unscented Kalman filter," *J. Aerosp. Eng.*, vol. 30, no. 6, Nov. 2017, Art. no. 04017063.
- [36] X. Wang, Y. Liang, Q. Pan, and F. Yang, "A Gaussian approximation recursive filter for nonlinear systems with correlated noises," *Automatica*, vol. 48, no. 9, pp. 2290–2297, 2012.
- [37] X. Wang, Y. Liang, Q. Pan, C. Zhao, and F. Yang, "Nonlinear Gaussian smoothers with colored measurement noise," *IEEE Trans. Autom. Control*, vol. 60, no. 3, pp. 870–876, Mar. 2015.
- [38] X. Wang, Y. Liang, Q. Pan, C. Zhao, and F. Yang, "Design and implementation of Gaussian filter for nonlinear system with randomly delayed measurements and correlated noises," *Appl. Math. Comput.*, vol. 232, pp. 1011–1024, Apr. 2014.
- [39] M. Roth, E. Özkan, and F. Gustafsson, "A student's t filter for heavy tailed process and measurement noise," in *Proc. IEEE Int. Conf. Acoust., Speech Signal Process.*, May 2013, pp. 5077–5774.
- [40] Y. L. Huang, Y. G. Zhang, N. Li, and J. Chambers, "Robust student's t based nonlinear filter and smoother," *IEEE Trans. Aerosp. Electron. Syst.*, vol. 52, no. 5, pp. 2586–2596, Oct. 2016.
- [41] S. Y. Cho and W. S. Choi, "Robust positioning technique in low-cost DR/GPS for land navigation," *IEEE Trans. Instrum. Meas.*, vol. 55, no. 4, pp. 1132–1142, Aug. 2006.
- [42] Z.-T. Zhang and J.-S. Zhang, "Sampling strong tracking nonlinear unscented Kalman filter and its application in eye tracking," *Chin. Phys. B*, vol. 19, no. 10, pp. 324–332, May 2010.
- [43] Q. Zhang, X. Meng, S. Zhang, and Y. Wang, "Singular value decomposition-based robust cubature Kalman filtering for an integrated GPS/SINS navigation system," *J. Navigat.*, vol. 68, no. 3, pp. 549–562, 2015.
- [44] R. Van der Merwe and E. A. Wan, "The square-root unscented Kalman filter for state and parameter-estimation," in *Proc. IEEE Int. Conf. Acoust., Speech, Signal Process.*, Salt Lake City, USA, May 2001, pp. 3461–3464.
- [45] G. Hu, S. Gao, Y. Zhong, B. Gao, and A. Subic, "Modified strong tracking unscented Kalman filter for nonlinear state estimation with process model uncertainty," *Int. J. Control.*, vol. 29, no. 12, pp. 1561–1577, Dec. 2015.
- [46] G. Hu, Y.-H. Liu, S.-S. Gao, and Y. Yang, "Improved strong tracking UKF and its application in INS/GPS integrated navigation," *J. Chin. Inertial Technol.*, vol. 22, no. 5, pp. 5634–5639, May 2014.
- [47] Q. Wang, "The theory and application research of adaptive-robust UKF for satellite integrated navigation system," *Huazhong Univ. Sci. Technol.*, Wuhan, China, Tech. Rep. 68–72, 2010.
- [48] S. Gao, G. Hu, and Y. Zhong, "Windowing and random weighting-based adaptive unscented Kalman filter," *Int. J. Adapt. Control Signal Process.*, vol. 29, no. 2, pp. 201–223, Feb. 2015.
- [49] Z. M. Durovic and B. D. Kovacevic, "Robust estimation with unknown noise statistics," *IEEE Trans. Autom. Control*, vol. 44, no. 6, pp. 1292–1296, Jun. 1999.
- [50] L. Chang, B. Hu, and G. Chang, "Multiple outliers suppression derivative-free filter based on unscented transformation," *J. Guid. Control Dyn.*, vol. 35, no. 6, pp. 1902–1907, Nov. 2012.
- [51] L. Chang, B. Hu, G. Chang, and A. Li, "Huber-based novel robust unscented Kalman filter," *IET Sci. Meas. Technol.*, vol. 6, no. 6, pp. 502–509, Nov. 2012.
- [52] B. Chen, X. Liu, H. Zhao, and J. C. Príncipe, "Maximum correntropy Kalman filter," *Automatica*, vol. 76, no. 2, pp. 70–77, Feb. 2017.
- [53] B. Chen and J. C. Príncipe, "Maximum correntropy estimation is a smoothed MAP estimation," *IEEE Signal Process. Lett.*, vol. 19, no. 8, pp. 491–494, Aug. 2012.
- [54] B. Chen, J. Wang, H. Zhao, N. Zheng, and J. C. Príncipe, "Convergence of a fixed-point algorithm under maximum correntropy criterion," *IEEE Signal Process. Lett.*, vol. 22, no. 10, pp. 1723–1727, Oct. 2015.
- [55] Y. Wang, W. Zheng, S. Sun, and L. Li, "Robust information filter based on maximum correntropy criterion," *J. Guid., Control, Dyn.*, vol. 39, no. 5, pp. 1126–1131, Jan. 2016.
- [56] R. Izanloo, S. A. Fakoorian, H. S. Yazdi, and D. Simon, "Kalman filtering based on the maximum correntropy criterion in the presence of non-Gaussian noise," in *Proc. Annu. Conf. Inf. Sci. Syst. (CISS)*, Mar. 2016, pp. 500–505.
- [57] B. Zhu, L. Chang, J. Xu, F. Zha, and J. Li, "Huber-based adaptive unscented Kalman filter with non-gaussian measurement noise," *Circuits, Syst., Signal Process.*, vol. 37, no. 9, pp. 3842–3861, Sep. 2018.
- [58] M. Manjunath and G. K. Shashidhar, "Segmentation and characterization of acoustic event spectrograms using singular value decomposition," *Expert Syst. Appl.*, vol. 120, pp. 413–425, Apr. 2019.
- [59] G. Liu, F. Worgotter, and I. Markelic, "Square-root sigma-point information filtering," *IEEE Trans. Autom. Control*, vol. 57, no. 11, pp. 2945–2950, Nov. 2012.

- [60] W. Zhou, J. Hou, L. Liu, T. Sun, and J. Liu, "Design and simulation of the integrated navigation system based on extended Kalman filter," *Open Phys.*, vol. 15, no. 1, pp. 182–187, Jan. 2017.
- [61] J. Dunik, M. Simandl, and O. Straka, "Unscented Kalman filter: Aspects and adaptive setting of scaling parameter," *IEEE Trans. Autom. Control*, vol. 57, no. 9, pp. 2411–2416, Sep. 2012.
- [62] Y.-L. Huang, Y.-G. Zhang, and Z.-M. Wu, "A high order unscented Kalman filtering method," *Acta Autom. Sinica*, vol. 40, no. 5, pp. 838–848, May 2014.



WEIDONG ZHOU received the bachelor's and master's degrees from the Harbin Institute of Technology, Harbin, China, in 1988 and 1991, respectively, and the Ph.D. degree from the College of Automation, Harbin Engineering University, Harbin, in 2016. In 2004, he visited Baco Company, Belgium and participated in many international academic conferences. He is currently a Professor of navigation, guidance, and control with Harbin Engineering University. His current research interests include signal processing, information fusion and their applications in navigation technology, such as inertial navigation and integrated navigation.



JIAXIN HOU received the B.S. degree from the Department of Automation, Northeast Petroleum University, Daqing, China, in 2006. He is currently pursuing the Ph.D. degree in control science and engineering with Harbin Engineering University, Harbin, China. His current research interests include signal processing, information fusion and their applications in navigation technology, such as inertial navigation and integrated navigation.

• • •